Strengthening mechanisms of clay building materials by starch

Julia Tourtelot, Jean-Baptiste d'Espinose de Lacaillerie, Myriam Duc, Jean-Didier Mertz, Ann Bourgès, Emmanuel Keita

Strengthening mechanisms of clay building materials by starch

Julia Tourtelot[1,2], Jean-Baptiste d'Espinose de Lacaillerie[3], Myriam Duc[4],

Jean-Didier Mertz[2], Ann Bourgès[5], Emmanuel Keita[1]*

[1]Laboratoire Navier, Université Gustave Eiffel, CNRS, ENPC, UMR8205, 77447 Marne la Vallée, France

[2] Laboratoire de Recherche des Monuments Historiques, Champs-sur-Marne, France;

[3] ESPCI ParisTech, PSL Research University, Sciences et Ingenierie de la matiere Molle, CNRS UMR7615, , F-75231 Paris Cedex 05, France

[4] GERS-SRO, Univ Gustave Eiffel, 77447 Marne la Vallée, France

[5] C2RMF, Centre de Recherche et de Restauration des Muse´es de France, France-Institut de Recherche Chimie Paris, PSL Research University, Chimie ParisTechCNRS, UMR8247, Paris 75005, France

Abstract.

Earth has a renewed interest in eco-friendly building materials. Starch is a promising additive, but its strengthening origin needs understanding to promote better solutions according to soil variability. This multiscale study examined natural clays and starches interactions. Clays and starches were evaluated based on mechanical and rheological properties. Kaolinite was found to be better reinforced by starches. At microscopic scale, starches modified the arrangement of grains and clays, but the role of botanical origin is unclear. At molecular scale, the ratio between amylose and amylopectin led the interactions with kaolinite. These results help to understand how bio-additives affect earth-based building materials.

1. Introduction

The development of low-carbon construction processes promotes the use of earth-based building materials [1–6]. Earth-based building materials can be described as natural concrete, composed of aggregates, such as sand or gravel, and a binder, clay minerals[7,8]. To be used in a more

standardized way, industries and researchers are interested in stabilizing earth-based building materials to increase their mechanical strength and durability [9–14].

From traditional recipes [15], starch has been identified as a promising additive[16]. Indeed, starch increases the mechanical behavior of earth-based building materials with only 1 wt% addition [17,18]. The stabilization of earth-based building materials with biopolymers is assumed to depend on the nature of the clay minerals by modifying mainly layer thickness and chemical composition [19–23]. It is also assumed that starch influences the rheology of fresh mixes depending on the clay nature of the earth-based building material [24]. Indeed, the behavior of mixes at the fresh state is a critical parameter for on-site applications [20,25].

Starches are biopolymers made from glucose found in cereals such as wheat, rice, or potato pulp. In their native form, the biopolymer chains are trapped in granules [26,27]. The granules must be exploded by heat in water to release the chains. Starch consists of two biopolymers: amylose and amylopectin. Amylose is a linear polymer, while amylopectin is a branched polymer. The ratio between the two molecules depends on the botanical source. The most common ratio is 20% of amylose and 80% of amylopectin but starches with high amylose or amylopectin content can be found [15,28–30]. Starches are often used as bioplastics, in industrial foods [31–33]. For instance, the amylose/amylopectin ratio was shown to be detrimental in adhesives for paper and wooden boards [34].

In order to develop the use of starch as an additive to earth-based building materials, it is essential to understand the mechanisms involved in its addition. Therefore, the interactions between clay minerals, the earth binder, and starches must be investigated. In traditional earth-based recipes, starches are mixed in a clay matrix, but the most advanced research in the literature referred to bioplastics application and the addition of clays in a starch matrix. The clay addition in these plastics improves their strength and reduces water vapor permeability [32,33,35]. For example, Wilhelm et al. showed a 72% increase in Young Modulus when 30% of clay is added to plasticize starch [35]. It has been shown that hydrogen bonds between starch polymer chains and clay particles are responsible for mechanical reinforcement [31–33,36]. However, starch bioplastics are plasticized [37] and sometimes stabilized with exfoliated clays to promote interactions [32,36]. Because of starches and clays modifications, these studies are not directly relevant to understand the mechanisms of starches in earth-based building materials. Thus, their conclusions, such as hydrogen bonds and polymer networks, cannot be directly applied without confirmation of natural clay minerals.

This study focuses on the interactions between natural clays and starches from the macroscopic to the molecular scale. Three representative natural clays and five botanical starch sources were used. The starch sources and their relevant dosages were evaluated based on mechanical and rheological properties at the macroscopic scale. At the microscopic scale, mercury porosimetry was assessed and the arrangement between grains and clays was observed to investigate the role of the botanical origin of the starches. Finally, at the molecular scale, the physicochemical interactions between starches and clays were investigated by spectroscopic means. This multiscale study allows a better understanding of the influence of bio-additives on earth-based building materials and improves mix-design.

2. Materials and methods

2.1. Materials

2.1.1. Clays and sand

Three clays were used: kaolinite supplied by SOKA (France), illite supplied by ARVEL (France), and montmorillonite supplied by ABM (Italy). They represent three characteristic groups of aluminum clays: TO structure for kaolinite, TOT non-swelling structure for illite, and TOT swelling structure for montmorillonite. The illite is in its potassium form, and the montmorillonite is calcic, while kaolinite hasn't any interlayer cation according to its structure.

The Atterberg limits and the cation exchange capacity (CEC) of these clays are presented in Table 1. The CEC was measured through exchange with hexamine cobalt, the liquid limit by the conventional method proposed by Casagrande, and the plastic limit by rolling out a thread [38].

Type of clay	**Liquid limit** ***Water content (wt%)***	**Plastic limit** ***Water content (wt%)***	**CEC** ***(meq/100g)***
Kaolinite	51	42	2
Illite	52	47	20
Montmorillonite	135	97	102

Table 1 : Atterberg limits of the three pure clays and their CEC

The XRD diffractograms allowed the identification of the mineral phases in the three clays (see Figure 1). In kaolinite clay, the major mineral phase is kaolinite, and the secondary mineral phases are illite and quartz. The illite clay contains kaolinite and illite minerals, with quartz and carbonates as secondary phases. Finally, the montmorillonite clay is composed of montmorillonite, with illite and quartz as secondary phases. The percentages of clay phases in these three clays were calculated [39] using a semi-quantitative method [40]. The semi-quantitative method determines the percentage of clay mineral phases according to the major peak area of each clay mineral on the XRD diffractogram. The kaolinite clay contains 84% kaolinite and 16% illite, while the illite clay contains 95% illite and 5% kaolinite. Finally, the montmorillonite clay is 99.3% montmorillonite and 0.7% illite.

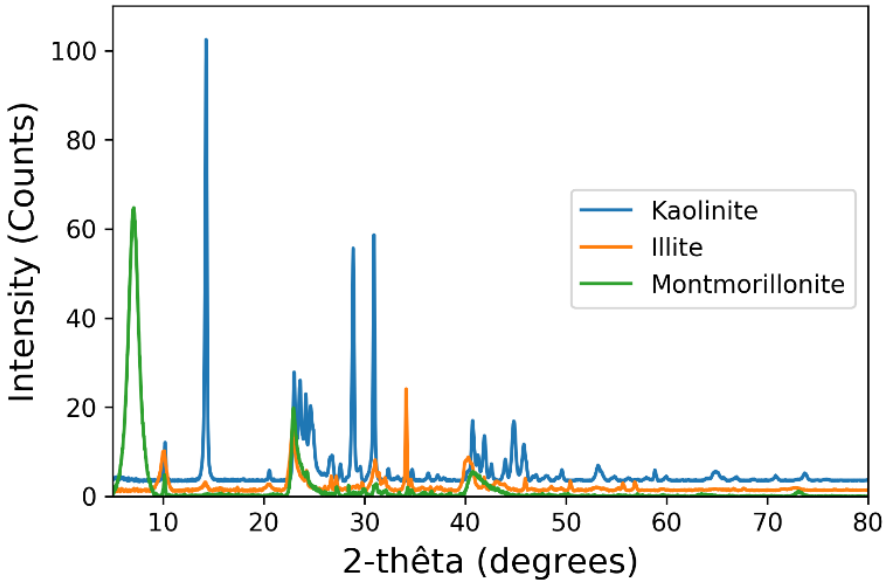

Figure 1 : XRD diffractograms of the three natural clays

The grain size distribution of the three clays was assessed by sedimentometry [18]. The sedimentometry test calculates the diameter of suspended clay particles under 80 µm applying the Stokes law. The clay particles were first deflocculated with a sodium hexametaphosphate solution. Kaolinite clay had the largest mineral particles compared to the illite and montmorillonite clays. To limit shrinkage of samples during drying, sand from "Sablières Palvadeau", France, was used. The particle size distribution, evaluated by sieving, ranges from 0 to 1 mm. Particle size distributions are presented for the mortar mixes in section 2.2.

2.1.2. Starches

Five starches were used in the present study of varying botanical origin and composition. The starches from maize (M), wheat (W), rice (R), and waxy maize (amylopectin - Ap) were purchased from Sigma-Aldrich. Starch from maize with high amylose content (amylose - Am) was also used. The five starches' size distribution was measured using a laser particle size analyzer (Malvern Mastersizer S) after heating at 90 °C in distilled water for 10 minutes; 5 minutes was enough to obtain uniform temperature; thus we chose to heat for 10 min. It shows particles between 10 and 50 μm.

Table 2 gives the mass percentage between amylose and amylopectin in the starches, as provided by producers. The starch from maize with high amylose content has the highest percentage of amylose at 72 %, followed by the starches from maize, wheat, and rice. Finally, the starch from waxy maize (amylopectin) has the lowest percentage of amylose. As a reminder, amylopectin is a branched polysaccharide with numerous hydroxyl groups, while amylose is a linear polysaccharide [15,28–30].

Botanical source of starch	**Amylose % mass**	**Amylopectin % mass**
Maize with high amylose content (amylose – Am)	72	28
Maize (M)	27	73
Wheat (W)	17	83
Rice (R)	13-25	75-87
Waxy maize (amylopectin – Ap)	1	99

Table 2 : Botanical origin of the five starches and their ratio between amylose and amylopectin

2.2. Sample preparation

The current study aims to study the interactions between clays and starches at different scales. For that purpose, two types of samples were designed: with and without sand. The sand was used to design mortars to obtain representative building materials without hiding the main effect of clay/starches interactions. Mixes with only clays and starches were used for the experiments at the molecular scale.

The present study aimed to investigate the origin of reinforcement mechanisms of clay materials with starches. A reference mortar mix was designed for each clay, with a sand/clay mass ratio equal to 70/30. The particle size distributions of the sand/clay mixes are plotted in Figure 2. In that mix, the

sand is used to structure the clay and not to design a mortar for construction applications. Thus, the particle size distribution shows the participation of sand and clay particles.

Moreover, each clay is sensitive to water differently, as shown by the liquidity and plasticity limits (Table 1). Thus, the amount of water was adapted for each one. The water-to-materials ratios were 13.6 wt%, 13.5 wt%, and 29.0 wt% for kaolinite, illite, and montmorillonite, respectively. Then, 1 wt% and 5 wt% of clay were replaced by starch, Table 3.

Mixe names	Clay (wt %)	Sand (wt %)	Starch (wt %)
Ref	30	70	0
1% of starch	29.7	70	0.3
5 % of starch	28.5	70	1.5

Table 3 : Compositions of the mortar mixes in percentage per weight

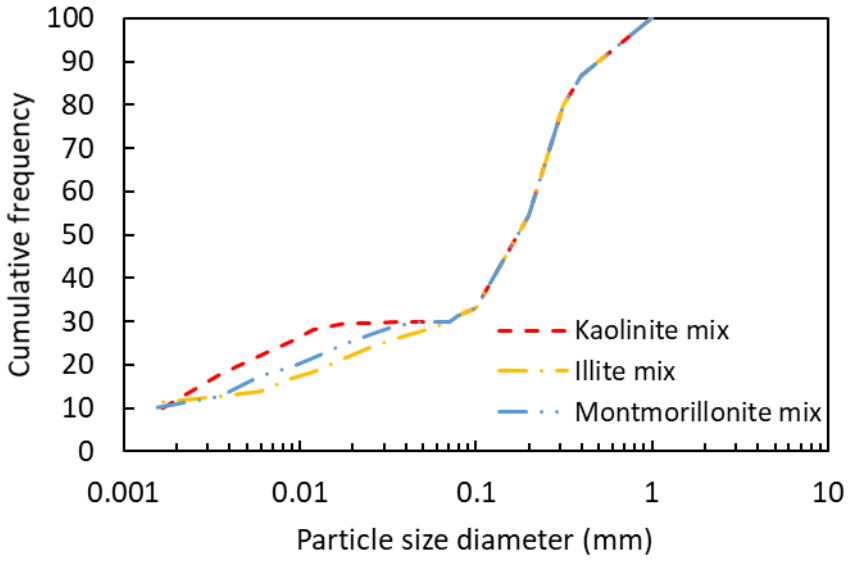

Figure 2 : Particle size distribution of reference mixes

All mortar samples were prepared following the same procedure. First, the clay and the sand were mixed by hand for 30 s. Then, the starch solution and the distilled water were poured into the powder mix and mixed in a planetary mixer at a constant speed of 62 rpm for 1 minute. After that, the bowl walls were scrapped, and a third mixing was performed at a constant speed of 93 rpm for 30 s. Finally, the mortar mixes were cured in hermetical beakers for a minimum of 48 h.

The molding procedure was adapted from Tiennot et *al.* [41]. The mortar mix was molded in a cylinder of 20 mm in diameter and 40 mm in height. Then, it was compacted until reaching uniaxial

stress of 44 kPa with a 1 mm/min displacement rate using an Instron® testing machine (Merlin 5500). After compaction and release from the mold, drying at 20 °C and 50 % HR was performed until a constant mass was reached.

For the preparation of the clay and starch mixes without sand, the composition and procedure of the mortar mixes were adapted. The clay, starch solution, and distilled water were mixed manually for 1 minute. Then the mixes were cured for 48 h in hermetical plastic bags. Finally, the mixes were dried in Petri dishes until constant weight at 20 °C and 50 %HR, without a molding step.

2.3. Experiments

2.3.1. Compressive test

The compressive strength and the elastic modulus of the mortar samples were evaluated using an unconfined uniaxial compressive test. The test was performed on a Shimadzu® AUTOGRAPH AGS-X press equipped with a 300 kN force sensor. The whole surface of samples is compressed by a 10 cm plate, larger than the sample diameter of 2 cm. The surfaces of the dried samples were flattened using a wood file to obtain samples with horizontal and parallel surfaces. The samples were compressed at a constant rate of 0.5 mm/min [42]. The equipment provided displacement and force. The compressive strength was considered from the maximal force before the failure of the sample. Finally, the elastic modulus was considered as the stress slope between 30% and 60% of the maximal stress on the linear strain part.

2.3.2. Weighted plunger test

The yield stress of the mortar mixes before molding was assessed with the weighted plunger test developed and presented in [43]. The weighted plunger test was performed with a standard plunger apparatus [44]. It consists of a container (70 mm high, diameter of 80 mm) with a cylindrical plunger tipped with a hemisphere (25 mm diameter). The plunger falls into the material inside the container, starting from the surface. The penetration distance of the plunger in the mortar is measured as a function of varying weights. The yield stress is defined as the ratio between the total forces and the immersed surfaces [43,45]. With the equipment used, the yield stress ranges from 6.6 kPa to 68 kPa.

2.3.3. Mercury porosimetry

Mercury Injection Porosimetry was used to measure the open porosity of mortar samples using the Autopore IV device from Micromeritics (USA). Connected porosity and pore size distribution were quantified from 300 to 0.003 µm, corresponding to a pressure applied to mercury from 0.0021 MPa to 0.1 MPa for the low-pressure unit and 0.1 MPa to 206 MPa for the high-pressure unit, considering the mercury surface tension and contact angle of 0.485 N/m and 136°, respectively. The mortar samples were dried at 60°C and sliced before measurement. Please note that the samples were not ground to keep the microstructure of the mortar.

2.3.4. Scanning Electron Microscopy (SEM)

Fractures of mortar samples were observed using a JEOL JSM IT300 with an Oxford Xmax50 probe. Morphology and structure were observed with a secondary electron detector with an accelerating voltage of 20 kV at High Vacuum. The magnifications used were x170 and x700.

2.3.5. Fourier transform infrared spectroscopy (FTIR)

The hydroxyl interactions between clays and starches were probed using FTIR spectroscopy. The analysis was performed by deposing a dried (60 °C) sample fragment on the diamond crystal on the bench. The device was a Total Attenuated Reflection ATR, Spotlight 100 Perkin Elmer, DTGS detector 4000 to 600 cm-1.

2.3.6. MAS NMR

^{1}H magic angle solid nuclear magnetic resonance (MAS NMR) spectra were acquired on a Bruker ASX500 spectrometer at 11.7 T. A 2.5 mm ZrO_2 rotor was used at a spinning frequency of 30 kHz. The ^{1}H spectra one-pulse were obtained at resonance frequencies of 500 MHz. Chemical shift values were referenced to tetramethylsilane (TMS). In the ^{1}H MAS NMR measurements, the pulse length was 2.8 µs and the recycle delay was 10 s.

3. Results

In order to identify the mechanisms of reinforcement of starches in earth-based building materials, ideal mortar mixes are prepared using specific clays. At the macroscopic scale, the specific behavior of starches will be evaluated in function of the nature of the clay in the mortars at two states: a dried one with a compressive test and a fresh one with yield stress measurements.

3.1. Compression strength and elastic modulus

The dry state of the mortar mixes was characterized by an unconfined compressive test for the macroscopic scale. The aim is to determine the enhancement of the mechanical strength by comparing the influence of starches on the compressive strength and the elastic modulus. Indeed, the mortar mix must be the most resistant to compression for minimal deformation before rupture.

Figure 3 presents the average compressive strength of the mortar samples. The compositions without starches are considered as references (Ref). References of illite and montmorillonite have a similar compressive strength of around 1 MPa, while reference of kaolinite has the lowest at 0.5 MPa.

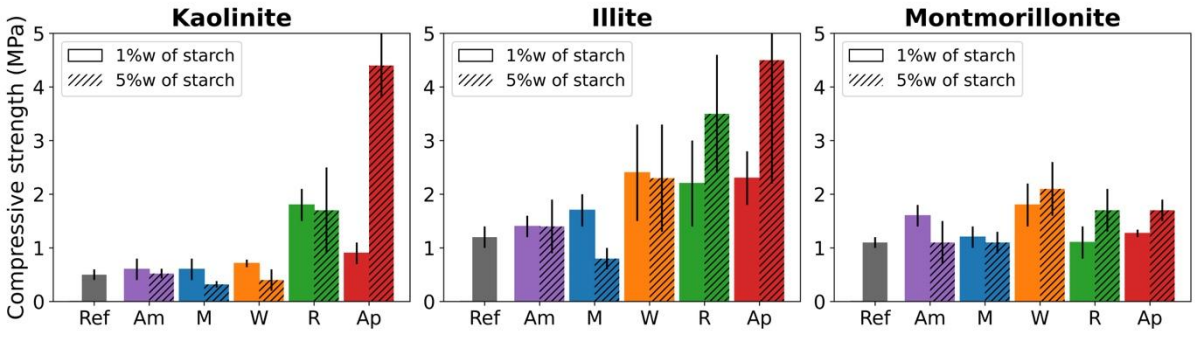

Figure 3 : Compressive strength of mortar mixes. From left to right: kaolinite, illite, and montmorillonite results. In grey: reference (Ref); purple: starch from maize with high amylose content (Am); blue: starch from maize (M); orange: starch from wheat (W); green: starch from rice (R); red: amylopectin (Ap)

Firstly, it can be noted that mechanical reinforcement by starches depends on the clay nature. Indeed, montmorillonite mortar is barely reinforced mechanically by starches (compressive strength remains between 1 and 2 MPa). However, illite mortar is consolidated mainly by wheat (W) and rice starches (R), as well as amylopectin (Ap). The compressive strength of illite mortar is increased by a

factor 2 to 4 with these three starches. As literature mentioned (Table 2), the ratio of amylose/amylopectin in rice can be very similar to wheat. The results obtained of illite may prove their similitude in composition and comfort with the significant role of amylopectin in the reinforcement process.

Finally, the kaolinite mortar is only reinforced by rice starch (R) and amylopectin (Ap) (Figure 3 left). With 1 wt% by mass, the compressive strength is multiplied by 2 with amylopectin (Ap) and 4 with rice starch (R). With 5 wt%, amylopectin (Ap) reinforces the most kaolinite mortar up to 4.5 MPa, multiplying the reference strength by 9. Thus, the compressive strength of kaolinite mortar increases three-fold with rice starch (R) and nine-fold with amylopectin (Ap).

The compressive strength of illite and kaolinite mortars increases four- to nine-fold with wheat starch (W), rice starch (R), and amylopectin (Ap). For an efficient reinforcement, the compressive strength increase might be combined with an increase in the elastic modulus. Indeed, large deformation may be detrimental to building structures. Then, the corresponding elastic moduli are presented in Figure 4 for the mortar mixes.

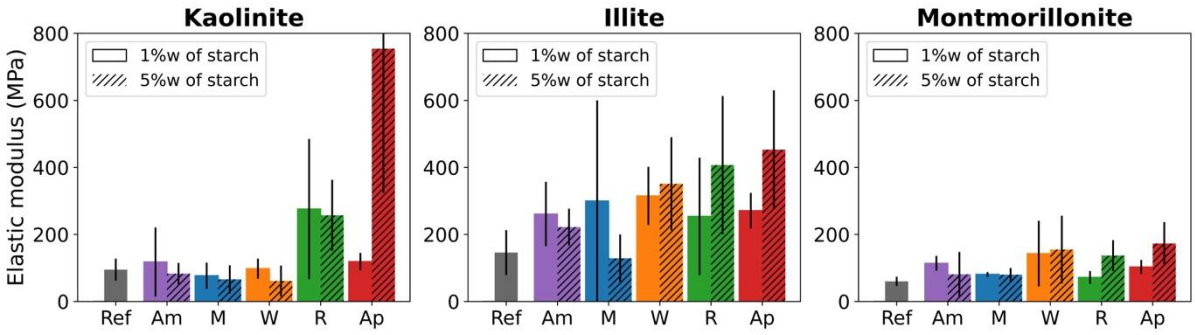

Figure 4 : Elastic modulus of mortar mixes. From left to right: kaolinite, illite, and montmorillonite results. In grey: reference (Ref); purple: starch from maize with high amylose content (Am); blue: starch from maize (M); orange: starch from wheat (W); green: starch from rice (R); red: amylopectin (Ap)

For montmorillonite mortar, results on elastic modulus are similar to the compressive strength, i.e., the elastic modulus of 60 MPa remains constant with the addition of starch. The elastic modulus of illite mortar increases with starch from 150 MPa for the reference (Ref) to 450 MPa with a 5 wt% of amylopectin (Ap). Finally, for kaolinite mortar, similar results for compressive strength are obtained, i.e., a significant increase in elastic modulus is observed with starches from 95 MPa to 280 MPa with 1 wt% of rice starch (R) and 760 MPa with 5 wt% of amylopectin (Ap).

Please note that the error bars are particularly high for some formulations compared to the reference formulas (Figure 3 and Figure 4). Two reasons may explain the dispersion of the error bars. Firstly, the addition of starch makes fresh mixes difficult to prepare and produces heterogeneous samples. Secondly, the confidence interval decreases with the number of tested samples, and more samples were tested for kaolinite and montmorillonite references (8 and 7 respectively), than other formulations (3 samples each).

The study of the dried mortar mixes at the macroscopic scale highlights that starches have various impacts on the mechanical properties according to the nature of the clay and starch. Kaolinite and illite exhibit the most disparity in mechanical behavior depending on the nature of starches.

3.2. Yield stress

The influence of starches in mortar mixes was also evaluated at the fresh state by measuring the yield stress. The yield stress corresponds to the threshold stress needed for the mortar to flow in the fresh mix. Ideally, to keep existing processes, increasing the strength at the dry state should not modify the mortar behavior at the fresh state. In this study, the yield stress of mortar mixes was assessed depending on the starch's nature and content. All the measurements were done at a constant water content for each clay. (Figure 5)

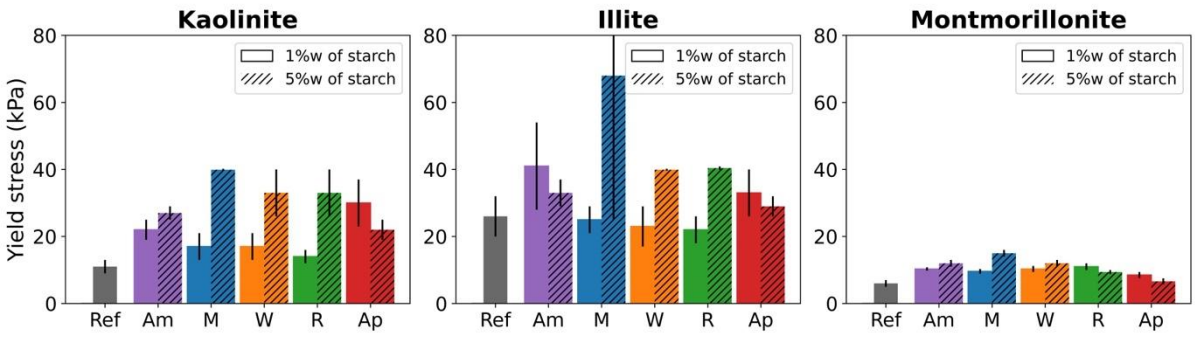

Figure 5 : Yield stress of mortar mixes. From left to right: kaolinite, illite, and montmorillonite results. In grey: reference (Ref); purple: starch from maize with high amylose content (Am); blue: starch from maize (M); orange: starch from wheat (W); green: starch from rice (R); red: amylopectin (Ap)

For Montmorillonite mortar, no significant effect was observed with the addition of 1% and 5% starch (Figure 5 Right). Reference montmorillonite mortar has the lowest yield stress at about 6 kPa, and it is lightly influenced by the starch addition with an increase up to 15 kPa with 5 wt% of maize

starch, indicating that starch does not contribute to the yield stress change. However, it should be noted that the water-to-clay ratio is high, close to one, so the starch concentration in water is between 1 and 5%.

Illite mortar has the highest yield stress at about 25 kPa without additives. At 1% concentration, no effect was observed on the yield stress, while at 5% concentration, the yield stress increased from 20 kPa to 40 kPa (Figure 5 Center). The results for maize starch were inconclusive due to large error bars. For starch from wheat and rice, error bars are small and the effect can be observed clearer than for maize starch and amylopectin. At 1%, due to the lower water-to-clay ratio than montmorillonite, the starch-to-water ratio was 2%, while water to clay ratio was approximately 50%. At 5%, this ratio leads to a starch concentration of 10% in water, which is significant, as starch dispersion in water may form a gel [26].

For kaolinite mortar, although the amounts of starch and water were similar to the illite formulation, an effect was observed with the addition of 1% of amylopectin and amylose (Figure 5 Left). The reference yield stress increased from 10 kPa to 20-40 kPa. At 5%, maize, rice and wheat starches increased the yield stress up to 40 kPa, but amylose yield stress remained around 20 kPa, close to the yield stress measured for 1% while amylopectin even decreased slightly the yield stress compared to the 1% value.

The mechanical tests, compression and measurement of the yield stress show a disparity in the results according to the nature of the clay and the starch. First, we observed that starches have a limited influence on the mechanics of montmorillonite. Second, we observed that starches reinforce mechanically illite and especially kaolinite. Rice starch (R) and amylopectin (Ap) increase the mechanical properties of illite and kaolinite. Furthermore, kaolinite is the most starch-strengthened clay compared to illite. To investigate the mechanisms of starch reinforcement, we focused on a comparative study between rice and maize starches mixed with kaolinite at microscopic and molecular scales.

3.3. Mercury porosimetry

Increasing the strength of building material is generally the consequence of better granular packing [46]. Thus, in order to explain the compressive results, we investigated the connected porosity, pore distribution, and granular arrangement of the mortars.

The connected porosity, accessible by mercury, was compared between the reference mortar (Kaol Ref) and with 1 and 5 wt% of maize (M) and rice (R) starch (Figure 6). The reference mortars had 26%

porosity, while bricks with maize starch (M) had 27% and rice starch (R) with 25% and 28% porosity at 1 and 5 wt% of starch, respectively. Considering the error bars, the comparison between the mortar mixes shows that moderated amounts of starches do not significantly influence the total porosity.

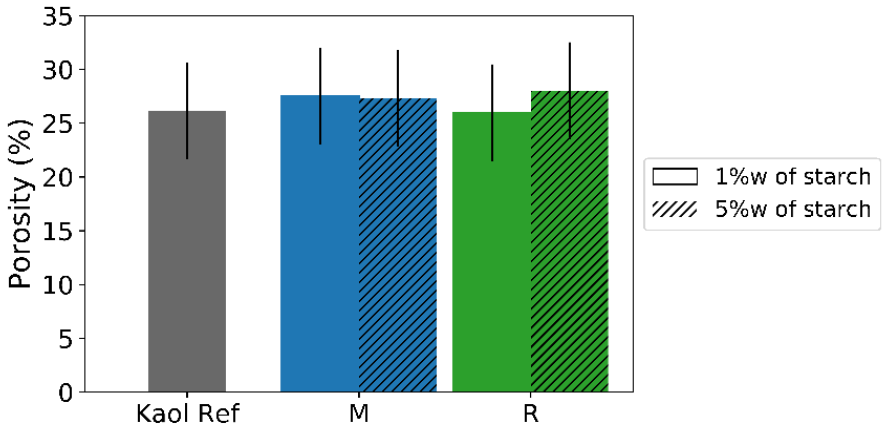

Figure 6 : Connected porosity accessible by mercury of kaolinite mortar mixes: reference (Kaol Ref), with starches from maize (M) and rice (R)

Besides connected porosity, the pore size distribution showed significant changes with starch addition (Figure 7). First, the reference sample containing kaolinite and sand presents two well-defined pore-size modes: the main mode centered at 0.2 µm associated with the pores inside the clay aggregates, and a minor mode at 1 µm associated with the pore spaces between the clay aggregates and the sand particles. Here, the limit between microporosity and macroporosity is considered at 0.5 µm.

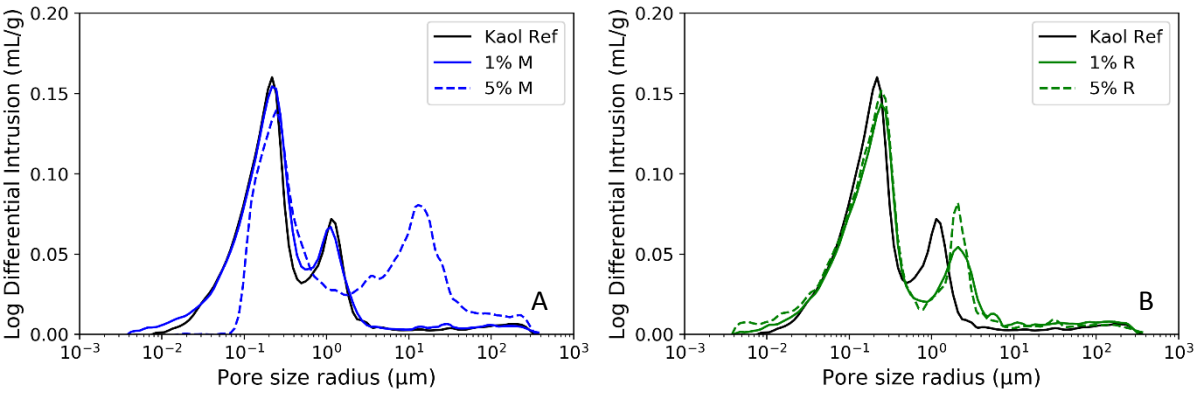

Figure 7 : Pore size radius distribution of kaolinite mortars. A: reference (Ref) and maize starch (M); B: reference (Ref) and rice starch(R)

In Figure 7, the pore size radius at 0.2 µm stays constant for both concentrations and both types of starch. Thus, the pore spaces inside the clay aggregates remain constant in kaolinite mortars and are unaffected by maize and rice starches. However, starches change the arrangement between the clay aggregates and the sand particles, which is measured as the macroporosity.

Indeed, in Figure 7 A, with 1 wt% of maize starch (1% M), the pore size radius remains constant around 1 µm, but with 5 wt% (5% M), the macroporosity distribution changes drastically: it is broadened with a maximum shifted to 15 µm. 5 wt% of maize starch (5% M) doubles the macropore volume with more polydispersity. This observation means that the macropores are bigger and destructured compared to the reference (Kaol Ref). Thus, 1 wt% of maize starch (1% M) does not influence the mortar structure, while 5 wt% of maize starch (5% M) modifies the microstructure of the mortar.

The influence of rice starch is different on the kaolinite mortar than maize starch (Figure 7 B). At both concentrations (1% R and 5% R), the pore radius slightly increases to 2 µm. These induced macropore spaces have an equivalent polydispersity to the reference mortar (Kaol Ref). Thus, rice starch increases the macroporosity without changing the arrangement of the structure. Then, the maize starch strongly modifies the microstructure of the mortar related to an increase in the macropore access size, while rice starch increases only the volume of these macropores.

3.4. SEM images

Figure 8 shows the arrangement between the particles in the kaolinite mortars with and without starch addition at two different scales in order to observe the clay/sand interaction identified by mercury porosimetry. In the reference kaolinite mortar (Figure 8 A and D), a sand grain can be identified in the clay bulk with clay particles at its surface. In addition, fractures can be noticed between the clay bulk and the sand grains (Figure 8 D).

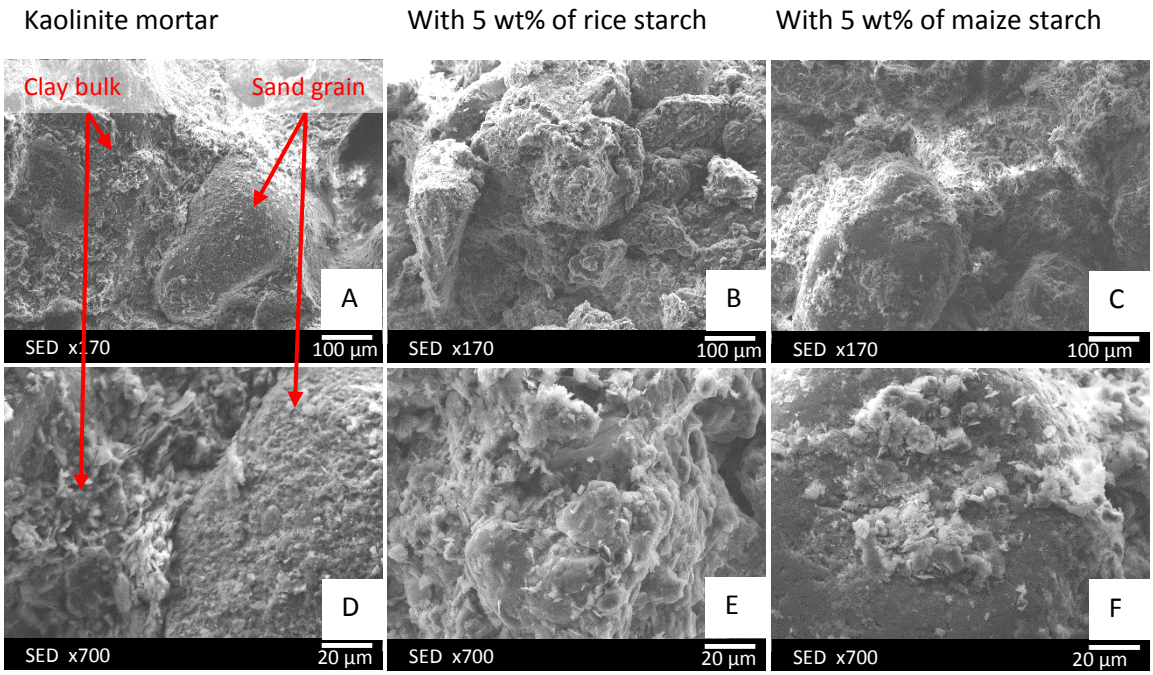

Figure 8 : SEM images of fracture surfaces of kaolinite mortars. A and D: reference mortar; B and E: with rice starch; C and F: with maize starch; at x170 and x700 of magnitude

With 5 wt% of rice starch (Figure 8 B and E), the surface texture of the clay bulk is modified. The clay particles are glued between each other and onto the sand grains giving a more homogeneous texture between the clay and the sand grains. Moreover, any cracks affect the contact between clay bulk and sand grains. On the opposite, with 5 wt% of maize starch (Figure 8 C and F), the mortar surface looks like the reference kaolinite mortar. The clay bulk and particles can be observed without the glued aspect.

The microscopic scale study of kaolinite mortars shows that the maize and rice starch influence the microstructure differently. The maize starch disrupts the macroporous arrangement of the mortars, while the rice starch seems to glue the clay particles between each other and onto the sand grains. Chemical interactions are expected between both components because their hydroxyl groups may be involved in hydrogen bonding. The following parts present analytical results obtained with clays and starch mixes without sand thanks to FTIR and NMR spectroscopies.

3.5. FTIR spectroscopy

The molecular interactions between kaolinite and starches were first investigated with FTIR spectroscopy on samples without sand. Figure 9 shows the infrared spectra of the raw materials and the kaolinite/starch mixes. Raw starches spectrums were performed with dried starch solutions and

prepared as used in the mixes and mortars. Figure 9 A and B focus on rice starch spectra, while Figure 9 C and D focus on maize starch. For all graphs, spectrums of raw components are presented: kaolinite, rice, and maize starches.

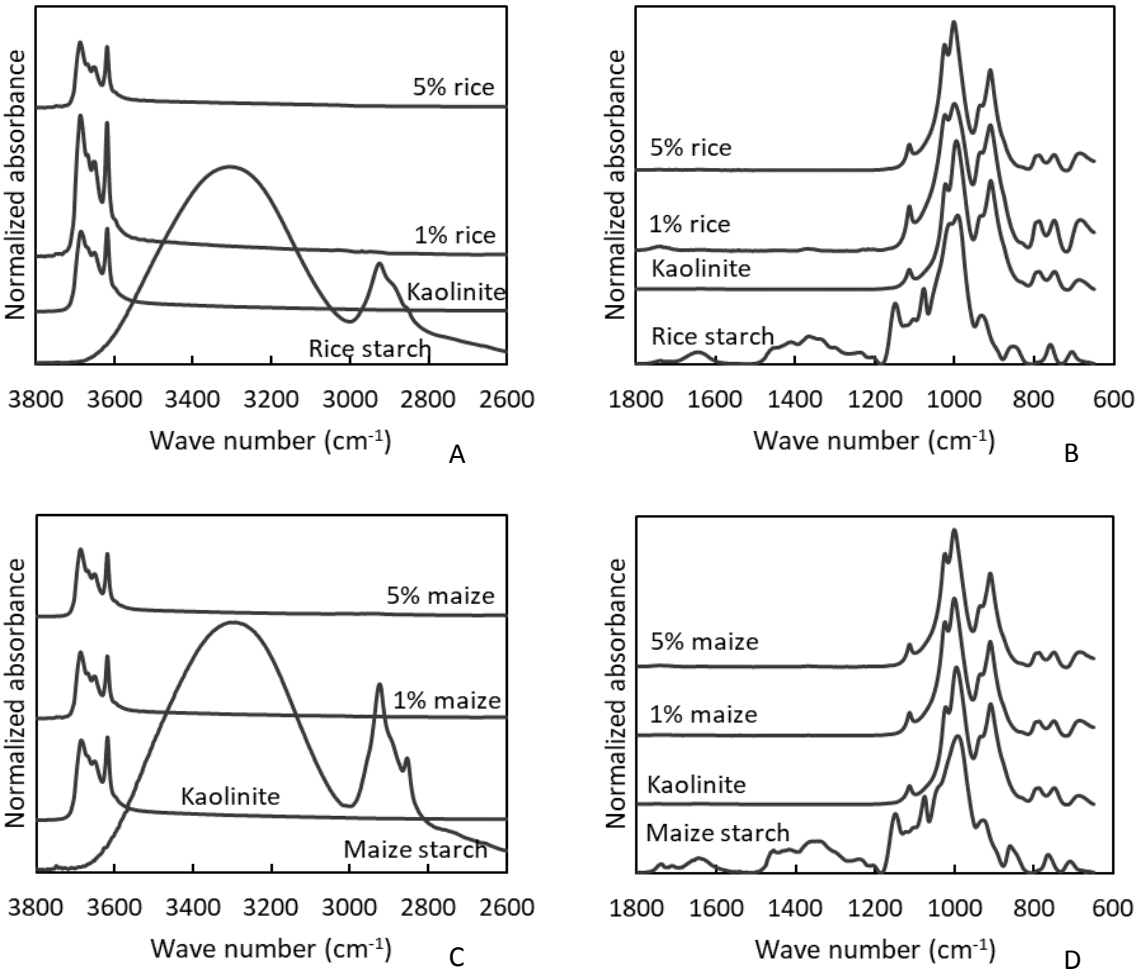

Figure 9 : FTIR spectra of raw components (kaolinite, maize, and rice starches) and mixes between kaolinite and starches. A and B: Rice starch spectra; C and D: Maize starch spectra

Firstly, all characteristic bands of the raw materials can be identified [47]. In the kaolinite raw spectra, we first identify the four bands corresponding to the OH stretching from 3685 to 3618 cm^{-1}. Then on the other part of the spectra, the bands from 1115 to 994 cm^{-1} correspond to the SiO deformation. The one at 994 cm^{-1} corresponds precisely to the apical SiO, i.e., the SiO localized between the octahedral and the tetrahedral layer of the kaolinite. Then, the bands at 936 and 910 cm^{-1} are for the deformation of Al_2OH bonds. The one at 794 cm^{-1} is characteristic of quartz. Finally, the ones at 750 and 689 cm^{-1} are for the elongation of the SiO bonds.

Raw starch spectra also exhibit classical bands [48]. The band at 3300 cm^{-1} corresponds to the OH bond stretching, while at 3000 cm^{-1}, it is the deformation of the CH_2 bonds. The bond at 1640 cm^{-1} corresponds to the adsorbed water. The 1350 and 1077 cm^{-1} bands are for the C-O-H bond, while the 1149 cm^{-1} band is for the C-O and C-C stretching. The C-H bonds are at 1014 and 856 cm^{-1}, while the band at 993 cm-1 is for the vibration of the glycosidic linkage. The 762 cm^{-1} band is for the C-C bond stretching, and the bands under 710 cm^{-1} correspond to the skeletal vibration mode of the pyranose ring.

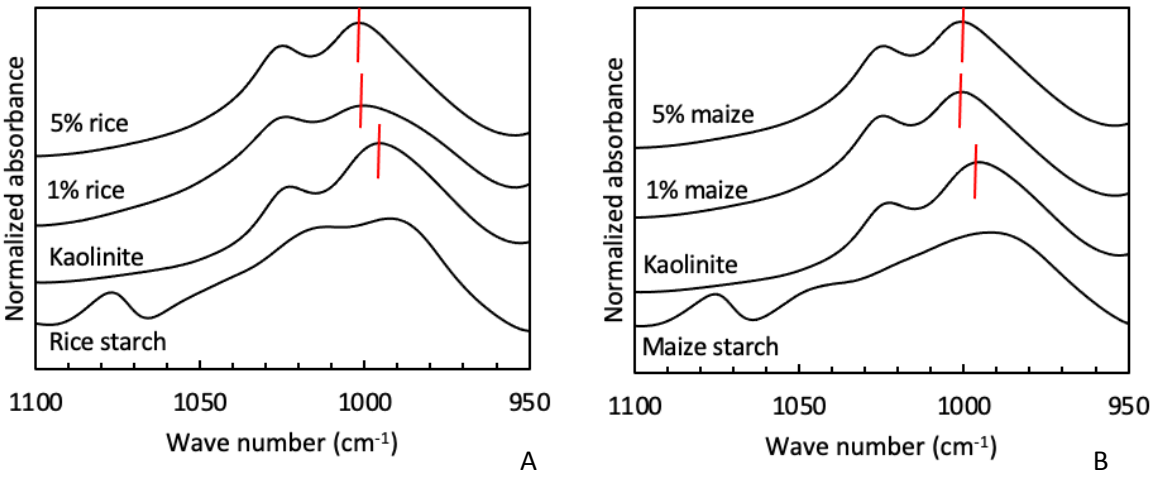

Figure 10 : Detailed FTIR spectra of raw components (kaolinite, maize, and rice starches) and mixes between kaolinite and starches. A with rice starch and B with maize starch

Mostly, when starches are added in small fractions to kaolinite, the kaolinite spectrum is found. There is a slight overall band shift from 1 to 2 cm^{-1}, but the apical SiO band, initially at 994 $cm^{-1,}$ undergoes a more critical shift from +6 to +8 cm^{-1} (Figure 10). This wavenumber increase means that the apical SiO bond is weakened. The chemical groups at the kaolinite surface are expected to undergo most of the modifications. Since the apical SiO bond is trapped in the layer, it is inductively influenced by the changes that the other accessible bonds on the kaolinite surface undergo [49]. Thus, this shift should correspond to a new chemical environment around the surfaces of the kaolinite sheets. This wavenumber shift can be observed for the maize and rice starch additions at both concentrations.

Finally, FTIR spectrums highlight the presence of hydrogen bonding between kaolinite surface and starches, but as FTIR is a qualitative analysis, the spectrums do not explain the differences in reinforcement (Figure 3 and Figure 4). Thus, a quantitative analysis focused on clay and starches

protons should be done to explain the different mechanical influences of maize and rice starches on kaolinite as ^{1}H MAS NMR spectroscopy.

3.6. ^{1}H MAS NMR spectroscopy

^{1}H MAS NMR measurements complete the FTIR results by refining the chemical interactions between kaolinite and starches in the mixes. Indeed, only protons are characterized with NMR spectroscopy, concentrating the range of observations on proton-mediated interactions such as hydrogen bonding. The measurements were done for the same samples as FTIR spectroscopy, i.e., for raw components (kaolinite, maize, and rice starches) and the mixes without sand. Raw starches spectrums were acquired with dried starch solutions. Figure 11 A focuses on maize starch spectra, while Figure 11 B focuses on rice starch spectra. Due to the lack of resolution, each component gives rise to only one broad resonance. Kaolinite characteristic chemical shift is around 2.4 ppm [50]; maize and rice starch shifts are about 4.3-4.4 ppm, respectively [51].

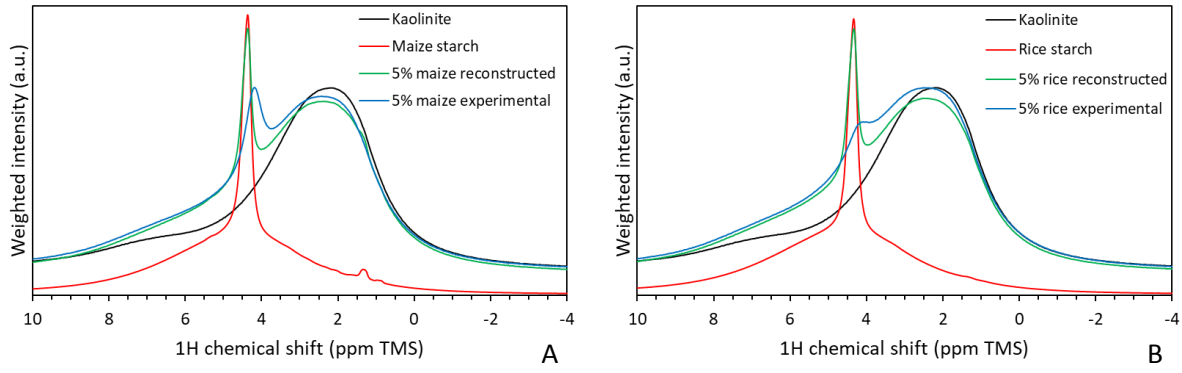

Figure 11 : ^{1}H MAS NMR spectra of raw components (kaolinite and dried starch gels) and mixes (reconstructed and experimental). A: Maize starch spectra; B: Rice starch spectra

Reconstructed spectra were plotted by summing the expected spectral contribution of the individual components (kaolinite and starch) weighted by their theoretical proton content and mass ratio in the mix. These reconstructed proton spectra (5% maize and 5% rice in green in Figure 11) thus correspond to hypothesis that the organic and inorganic phases are mixed and do not interact. The starch resonance peak is sharp and higher than the kaolinite resonance peak. Comparison of these reconstructed and experimental spectra is expected to reveal proton-mediated interactions, such as hydrogen bonding. At the resonance peak of kaolinite, the experimental spectra follow the reconstructed ones, while the resonance peak of rice starch is more pronounced than maize starch. Indeed, in the experimental spectra of Figure 11 (blue curves), the resonance peak of the maize

starch protons is broadened but its intensity is preserved in the mix with kaolinite (A), whereas the resonance peak of starch disappears for rice in the presence of kaolinite (B). This suggests a more significant change in the chemical environment of the rice starch protons when mixed with kaolinite.

4. Discussion

The addition of starch to earth-based building materials is a widely used stabilization technique. A previous laboratory study showed that starch added to the fresh mix improves the mechanical properties of earth-based building materials[16]. In the present paper, we worked with simplified materials to understand the phenomenon. Thus, we investigated the interactions between natural clays and starches, ranging from the macroscopic to the molecular scale and varying the botanical source of starch, so the ratio amylose/amylopectin. The principal result is that kaolinite and illite are reinforced with rice starch and amylopectin, mainly at 5 wt%. The comparison between maize and rice starch, which may have a different amylose/amylopectin ratio and different effects on mechanical properties, showed the presence of hydrogen bonding between starch and clay, with a greater effect of rice starch than maize starch.

4.1. Fresh State

This study aims to verify that the addition of starch to the simplified materials improves their mechanical properties and to identify the physicochemical origin. However, when formulating earth-based building materials, the rheological behavior must be considered to ensure workability in the fresh state [4]. Then, the goal is to improve strength but workability at fresh state should be kept to mold the samples.

Moreover, fresh state modifications could indicate particle interaction changes [52,53]. Indeed, a high yield stress increase may result from the interactions between starch and kaolinite, reinforcing the percolated solid network [43,52,53]. However, for amylose at 5%, yield stress remained around 20 kPa, close to the yield stress measured for 1% and for amylopectin, even the yield stress decreased slightly between 1% and 5% (Figure 5). These high yield stresses may be due to the interaction of starch with the kaolinite reinforcing the percolated matrix. At 5%, the interaction between kaolinite and starch and the gelation of starch could potentially create opposite behaviors. Maize, rice, and wheat starches significantly increased the yield stress, while amylose and amylopectin maintained the same yield stress at 1% (Figure 5 Left).

No clear correlation between fresh state and mechanical behavior could be obtained except for amylopectin. A rheological and physicochemical study of the clay/starch suspension, which is out of

the scope of this paper, should complete the analysis to correlate fresh state behavior fully and dried compressive strength. In this paper, the most effective starch sources for increasing strength while maintaining workability at the fresh state are those with the smallest yield stress increase; i.e. rice starch and amylopectin.

4.2. Hardened State

This study investigated the mechanical and physicochemical effects of adding starch to simplified mortar mixtures consisting of clay, sand, and starch. From a macroscopical point of view, the results showed no effect on the samples where the clay was montmorillonite. However, certain starches significantly increased the mechanical strength of mortars made of illite and kaolinite (see Figure 3). Results on elastic modulus were less conclusive due to high dispersion of the measurements (see Figure 4). Rice and amylopectin starches were found to significantly increase the adobe compressive strength, while maize starch did not modify the strength significantly.

The mechanical behavior induced by the starches can be explained partially by the microstructural changes, with maize starch increasing the macropore size and rice starch consolidating the kaolinite mortar (see Figure 7).

At the molecular scale, Infrared and RMN spectroscopic measurements showed changes in the chemical environments of kaolinite and starches in the mixes. IR spectroscopy showed that the kaolinite surface was indirectly chemically modified in the presence of starches, maize, and rice (see Figure 10). 1H MAS NMR spectroscopy showed a difference in interaction with kaolinite for maize and rice, indicating that rice starch protons in the presence of kaolinite are involved in an additional interaction compared to kaolinite reference, while for maize starch, the starch proton did not interact with the kaolinite ones (see Figure 11).

We suggest that the increase of mechanical strength due to starches lies in a high sensitivity to the amount of amylopectin (Table 2). Initially, we could assume that the amount of amylopectin between maize starch (73 wt%), rice (75 to 87 wt%) and wheat (83 wt%) would be similar. However, rice starch increases mechanical strength (see Figure 3), whereas wheat and maize starches don't affect mechanical properties. Therefore, a content of amylopectin over 80% may be a key parameter to increase mechanical properties. In this study, rice starch may contain more than 83 wt% of amylopectin or the botanical starch may lead to higher affinity with kaolinite. Thus, the greater amount of amylopectin **could** explain the greater presence of hydrogen bonding in the rice starch/kaolinite mix. Indeed, this interpretation requires further work to be confirmed, especially a precise determination of the ratio of the two polymers within starches. Moreover, further study

should be done to separate the effect of the amylose/amylopectin ratio and the botanical source of the starch. For illite, the reinforcement by amylopectin appears at a much smaller magnitude (see Figures 3, 4, 5). In fact, the illite clay contains kaolinite as a secondary mineral, and the same strengthening increased by amylopectin follow the same trend between kaolinite and illite-based mortars. Then, the complete absence of kaolinite minerals in the montmorillonite clay would explain why starches did not modify the compressive strength and modulus of elasticity of montmorillonite-based mortars.

5. Practical consequences

The practical consequences for the straightforward improvement of earth-based building materials are mitigated, as the strengthening of the clay is dependent on the botanical origin of the starch and the mineral composition of the clay, which is not always possible to measure for local resources. For montmorillonite, the conclusion is clear: mortar properties are not influenced by starch addition. Kaolinite mortars are improved by starch with a high amylopectin fraction. For mixed clays, mortar properties may increase slightly by adding starches.

Our findings indicate that the botanical origins of the starch play a significant role in strengthening the clay. Additionally, the mineral composition of the clay is an important parameter that should be taken into account, and laboratory characterizations like XRD should be correlated to field measurements on local resources. For instance, on-field test could be developed to establish the presence of kaolinite.

Furthermore, the simple idea of an additive interacting with the clay does not hold, as the additive may also modify porosity. Finally, the impact on the fresh state should not be underestimated, as earth-based building materials are processed with low energy, and high yield stress may prevent homogeneous on-site mixing and processing. Given the identified barriers to the generalization of using starch to reinforce earth-based building materials, it is not surprising that there is a wide variety of additives used to reinforce clay-based materials across the world, they are the results of trade-off between workability, strengthening and botanical and earth variabilities.

6. Conclusion

To study the interactions between natural clays and starches, we used mortars made out of kaolinite, illite and montmorillonite and tested five botanical sources of starch. In this study, each clay kind and the specific botanic source for starch composition are considered individually. Earth reinforcement is not as easy as it can be assumed, and materials, earth, or biopolymers are different and complex in

mineralogy or chemistry. As kaolinite samples were better reinforced than the other clays, the microscopic investigations focused on kaolinite with rice and maize starch. The porosimetry analysis showed a modification of grain arrangement and clays with additives compared to the reference. At the molecular scale, rice starch seemed to interact more strongly with kaolinite than maize. These molecular differences should be at the origin of the higher mechanical strength for macroscopical samples of kaolinite with rice addition in comparison to maize ones. Finally, a straightforward generalization of these results seems still complicated as some new investigations are needed regarding kaolinite and amylopectin threshold. The reinforcement depends strongly on the variability of the clay components and the botanical sources; further studies are required to define more precisely the composition thresholds, such as varying amylose/amylopectin ratios for the same source.

7. Acknowledgments

This work has been carried out within the frame of the project Alluvium. Initiated in 2018, Alluvium is part of I-SITE FUTURE, a French initiative to answer the challenges of sustainable cities. We acknowledge the help of Jérémie Hénin for the SEM measurements.

8. Funding

This study was funded by I-SITE FUTURE from the French Research Agency (project name: Alluvium).

9. Bibliography

[1] J.C. Morel, R. Charef, E. Hamard, A. Fabbri, C. Beckett, Q.B. Bui, Earth as construction material in the circular economy context: practitioner perspectives on barriers to overcome, Philosophical Transactions B. (2021). https://doi.org/https://doi.org/10.1098/rstb.2020.0182.

[2] H. Van Damme, H. Houben, Earth concrete. Stabilization revisited, Cem Concr Res. 114 (2018) 90–102. https://doi.org/10.1016/j.cemconres.2017.02.035.

[3] F. Pacheco-Torgal, S. Jalali, Earth construction: Lessons from the past for future eco-efficient construction, Constr Build Mater. 29 (2012) 512–519. https://doi.org/10.1016/j.conbuildmat.2011.10.054.

[4] D. Gallipoli, A.W. Bruno, C. Perlot, J. Mendes, A geotechnical perspective of raw earth building, Acta Geotech. 12 (2017) 463–478. https://doi.org/10.1007/s11440-016-0521-1.

[5] A. Brás, A. Antunes, A. Laborel-Préneron, R. Ralegaonkar, A. Shaw, M. Riley, P. Faria, Optimisation of bio-based building materials using image analysis method, Constr Build Mater. 223 (2019) 544–553. https://doi.org/10.1016/j.conbuildmat.2019.06.148.

[6] A. Ventura, C. Ouellet-Plamondon, M. Röck, T. Hecht, V. Roy, P. Higuera, T. Lecompte, P. Faria, E. Hamard, J.-C. Morel, G. Habert, Environmental Potential of Earth-Based Building Materials: Key Facts and Issues from a Life Cycle Assessment Perspective, in: J.-C. and A.J.-E. and B.Q.-B. and G.D. and R.B.V.V. Fabbri Antonin and Morel (Ed.), Testing and Characterisation of Earth-Based Building Materials and Elements: State-of-the-Art Report of the RILEM TC 274-TCE, Springer International Publishing, Cham, 2022: pp. 261–296. https://doi.org/10.1007/978-3-030-83297-1_8.

[7] D. Ardant, C. Brumaud, A. Perrot, G. Habert, Robust clay binder for earth-based concrete, Cem Concr Res. 172 (2023) 107207. https://doi.org/10.1016/j.cemconres.2023.107207.

[8] G. Landrou, C. Brumaud, G. Habert, Clay particles as binder for earth buildings materials: a fresh look into rheology of dense clay suspensions, EPJ Web Conf. 140 (2017) 13010. https://doi.org/10.1051/epjconf/201714013010.

[9] A. Seco, J.M. del Castillo, C. Perlot, S. Marcelino-Sádaba, E. Prieto, S. Espuelas, Experimental Study of the Valorization of Sulfate Soils for Use as Construction Material, Sustainability. 14 (2022) 6609. https://doi.org/10.3390/su14116609.

[10] S. Muguda, P.N. Hughes, C.E. Augarde, C. Perlot, A. Walter Bruno, D. Gallipoli, Cross-linking of biopolymers for stabilizing earthen construction materials, Building Research & Information. 50 (2022) 502–514. https://doi.org/10.1080/09613218.2021.2001304.

[11] A. Romano, H. Mohammed, V. Torres de Sande, A. Bras, Sustainable bio-based earth mortar with self-healing capacity, Proceedings of the Institution of Civil Engineers - Construction Materials. 174 (2021) 3–12. https://doi.org/10.1680/jcoma.19.00090.

[12] S. Guihéneuf, D. Rangeard, A. Perrot, Cast, compaction, vibro-compaction or extrusion: processing methods for optimizing the mechanical strength of raw earth-based

materials, Academic Journal of Civil Engineering. 37 (2019) 156–163. https://doi.org/10.26168/icbbm2019.22.

[13] D. Gallipoli, A.W. Bruno, Q.-B. Bui, A. Fabbri, P. Faria, D. V. Oliveira, C. Ouellet-Plamondon, R.A. Silva, Durability of Earth Materials: Weathering Agents, Testing Procedures and Stabilisation Methods, in: J.-C. and A.J.-E. and B.Q.-B. and G.D. and R.B.V.V. Fabbri Antonin and Morel (Ed.), Testing and Characterisation of Earth-Based Building Materials and Elements: State-of-the-Art Report of the RILEM TC 274-TCE, Springer International Publishing, Cham, 2022: pp. 211–241. https://doi.org/10.1007/978-3-030-83297-1_6.

[14] A. Antunes, P. Faria, V. Silva, A. Brás, Rice husk-earth based composites: A novel bio-based panel for buildings refurbishment, Constr Build Mater. 221 (2019) 99–108. https://doi.org/https://doi.org/10.1016/j.conbuildmat.2019.06.074.

[15] R. Anger, L. Fontaine, Interactions argiles/biopolymères : Patrimoine architectural en terre et stabilisants naturels d'origine animale et végétale, 2013.

[16] J. Tourtelot, A. Bourgès, E. Keita, Influence of Biopolymers on the Mechanical Behavior of Earth-Based Building Materials, Recent Prog Mater. 03 (2021) 1–1. https://doi.org/10.21926/rpm.2103031.

[17] G. Alhaik, M. Ferreira, V. Dubois, E. Wirquin, S. Tilloy, E. Monflier, G. Aouad, Enhance the rheological and mechanical properties of clayey materials by adding starches, Constr Build Mater. 139 (2017) 602–610. https://doi.org/10.1016/j.conbuildmat.2016.11.130.

[18] Q.Q. Pei, X.D. Wang, L.Y. Zhao, B. Zhang, Q.L. Guo, A sticky rice paste preparation method for reinforcing earthen heritage sites, J Cult Herit. 44 (2020) 98–109. https://doi.org/10.1016/j.culher.2020.01.009.

[19] A. Perrot, D. Rangeard, F. Menasria, S. Guihéneuf, Strategies for optimizing the mechanical strengths of raw earth-based mortars, Constr Build Mater. 167 (2018) 496–504. https://doi.org/10.1016/j.conbuildmat.2018.02.055.

[20] S. Guihéneuf, D. Rangeard, A. Perrot, Processing methods for optimising the mechanical strength of raw earth-based materials, Proceedings of Institution of Civil

Engineers: Construction Materials. 174 (2021) 150–160. https://doi.org/10.1680/jcoma.19.00115.

[21] D. Ardant, C. Brumaud, G. Habert, Influence of additives on poured earth strength development, Materials and Structures/Materiaux et Constructions. 53 (2020) 1–17. https://doi.org/10.1617/s11527-020-01564-y.

[22] S.J. Armistead, C.C. Smith, S.S. Staniland, Sustainable biopolymer soil stabilisation: the effect of microscale chemical characteristics on macroscale mechanical properties, Acta Geotech. (2022). https://doi.org/10.1007/s11440-022-01732-0.

[23] R.A. Mikofsky, S.J. Armistead, W. V. Srubar, On the Bonding Characteristics of Clays and Biopolymers for Sustainable Earthen Construction, RILEM Bookseries. 45 (2023) 280–292. https://doi.org/10.1007/978-3-031-33465-8_22/COVER.

[24] G. Alhaik, V. Dubois, E. Wirquin, A. Leblanc, G. Aouad, Evaluate the influence of starch on earth/hemp or flax straws mixtures properties in presence of superplasticizer, Constr Build Mater. 186 (2018) 762–772. https://doi.org/10.1016/j.conbuildmat.2018.07.209.

[25] M. Lagouin, A. Laborel-Préneron, C. Magniont, S. Geoffroy, J.-E. Aubert, Effects of organic admixtures on the fresh and mechanical properties of earth-based plasters, Journal of Building Engineering. 41 (2021) 102379. https://doi.org/https://doi.org/10.1016/j.jobe.2021.102379.

[26] R.F. Tester, J. Karkalas, X. Qi, Starch—composition, fine structure and architecture, J Cereal Sci. 39 (2004) 151–165. https://doi.org/10.1016/j.jcs.2003.12.001.

[27] M. Sujka, J. Jamroz, Ultrasound-treated starch: SEM and TEM imaging, and functional behaviour, Food Hydrocoll. 31 (2013) 413–419. https://doi.org/10.1016/j.foodhyd.2012.11.027.

[28] J.J.M. Swinkels, Composition and Properties of Commercial Native Starches, Starch - Stärke. 37 (1985) 1–5. https://doi.org/10.1002/star.19850370102.

[29] S. Pérez, E. Bertoft, The molecular structures of starch components and their contribution to the architecture of starch granules: A comprehensive review, Starch - Stärke. 62 (2010) 389–420. https://doi.org/10.1002/star.201000013.

[30] M. Seguchi, T. Higasa, Tomohiko Mori, Study of wheat starch structures by sonication treatment, Cereal Chem. 71 (1994) 636–639.

[31] H. Liu, D. Chaudhary, S. Yusa, M.O. Tadé, Glycerol/starch/Na+-montmorillonite nanocomposites: A XRD, FTIR, DSC and 1H NMR study, Carbohydr Polym. 83 (2011) 1591–1597. https://doi.org/10.1016/j.carbpol.2010.10.018.

[32] J.A. Mbey, S. Hoppe, F. Thomas, Cassava starch–kaolinite composite film. Effect of clay content and clay modification on film properties, Carbohydr Polym. 88 (2012) 213–222. https://doi.org/10.1016/j.carbpol.2011.11.091.

[33] A. Orsuwan, R. Sothornvit, Development and characterization of banana flour film incorporated with montmorillonite and banana starch nanoparticles, Carbohydr Polym. 174 (2017) 235–242. https://doi.org/10.1016/j.carbpol.2017.06.085.

[34] P. Liu, J. Ling, T. Mao, F. Liu, W. Zhou, G. Zhang, F. Xie, Adhesive and Flame-Retardant Properties of Starch/Ca2+ Gels with Different Amylose Contents, Molecules. 28 (2023) 4543. https://doi.org/10.3390/MOLECULES28114543/S1.

[35] H.-M. Wilhelm, M.-R. Sierakowski, G.P. Souza, F. Wypych, Starch films reinforced with mineral clay, Carbohydr Polym. 52 (2003) 101–110. https://doi.org/10.1016/S0144-8617(02)00239-4.

[36] J.A. Mbey, F. Thomas, Components interactions controlling starch–kaolinite composite films properties, Carbohydr Polym. 117 (2015) 739–745. https://doi.org/10.1016/j.carbpol.2014.10.053.

[37] L. Avérous, P.J. Halley, Biocomposites based on plasticized starch, Biofuels, Bioproducts and Biorefining. 3 (2009) 329–343. https://doi.org/10.1002/bbb.135.

[38] ISO 17892-12:2018 - Geotechnical investigation and testing — Laboratory testing of soil — Part 12: Determination of liquid and plastic limits, (2018).

[39] C. Chen, A mineralogical approach to use the non-qualified fine aggregates in asphalt concrete pavement, Université Paris-Est, 2016.

[40] T. Holtzapffel, Les minéraux argileux. Préparation. Analyse diffractométrique et détermination., Université des Sciences et Techniques de Lille 1, 1985.

[41] M. Tiennot, J.-D. Mertz, A. Bourgès, A. Liégey, A. Chemmi, A. Bouquillon, Ethyl Silicate for Unbaked Earth Tablets Conservation: Evaluation of the Physico-mechanical Aspects, Studies in Conservation. 65 (2020) 285–295. https://doi.org/10.1080/00393630.2020.1715057.

[42] ISO 17892-7:2018 - Geotechnical investigation and testing - Laboratory testing of soil - Part 7 : unconfined compression test, (2018).

[43] J. Tourtelot, I. Ghattassi, R. Le Roy, A. Bourgès, E. Keita, Yield stress measurement for earth-based building materials: the weighted plunger test, Mater Struct. 54 (2021) 6. https://doi.org/10.1617/s11527-020-01588-4.

[44] NF EN 413-2 - Ciment à maçonner — Partie 2 : Méthodes d'essai, (2017).

[45] D. Lootens, P. Jousset, L. Martinie, N. Roussel, R.J. Flatt, Yield stress during setting of cement pastes from penetration tests, Cem Concr Res. 39 (2009) 401–408. https://doi.org/10.1016/j.cemconres.2009.01.012.

[46] F. de Larrard, Concrete mixture proportioning : a scientific approach, E & FN Spon, 1999. https://books.google.fr/books?hl=fr&lr=&id=tXHjwTa0_tkC&oi=fnd&pg=PR10&dq=de+larrard+francois&ots=TvolH_J39X&sig=0Domh8qDEG0v1obQFu5B89Tb0lU#v=onepage&q=de%20larrard%20francois&f=false (accessed October 11, 2017).

[47] J. Madejová, W.P. Gates, S. Petit, IR Spectra of Clay Minerals, in: Dev Clay Sci, 2017: pp. 107–149. https://doi.org/10.1016/B978-0-08-100355-8.00005-9.

[48] R. Kizil, J. Irudayaraj, K. Seetharaman, Characterization of Irradiated Starches by Using FT-Raman and FTIR Spectroscopy, J Agric Food Chem. 50 (2002) 3912–3918. https://doi.org/10.1021/jf011652p.

[49] B.C. Smith, Fundamentals of Fourier Transform Infrared Spectroscopy, CRC Press, 2011. https://doi.org/10.1201/b10777.

[50] S. Hayashi, T. Ueda, K. Hayamizu, E. Akiba, NMR study of kaolinite. 1. Silicon-29, aluminum-27, and proton spectra, J Phys Chem. 96 (1992) 10922–10928. https://doi.org/10.1021/j100205a058.

[51] F.H. Larsen, A. Blennow, S.B. Engelsen, Starch Granule Hydration—A MAS NMR Investigation, Food Biophys. 3 (2008) 25–32. https://doi.org/10.1007/s11483-007-9045-4.

[52] P. Coussot, Rheophysics, Springer International Publishing, Cham, 2014. https://doi.org/10.1007/978-3-319-06148-1.

[53] J. Hot, H. Bessaies-Bey, C. Brumaud, M. Duc, C. Castella, N. Roussel, Adsorbing polymers and viscosity of cement pastes, Cem Concr Res. 63 (2014) 12–19. https://doi.org/10.1016/j.cemconres.2014.04.005.